ELSEVIER

Contents lists available at ScienceDirect

Composite Structures

journal homepage: www.elsevier.com/locate/compstruct



A multiscale model to study the enhancement in the compressive strength of multi-walled CNT sheet overwrapped carbon fiber composites



Pruthul Kokkada Ravindranath^{a,*}, Samit Roy^a, Vinu Unnikrishnan^c, Xuemin Wang^d, Tingge Xu^b, Ray Baughman^e, Hongbing Lu^b

- ^a Aerospace Engineering and Mechanics Department, University of Alabama, Tuscaloosa, AL, USA
- ^b Department of Mechanical Engineering, University of Texas at Dallas, Richardson, TX, USA
- School of Engineering, Computer Science and Mathematics, West Texas A&M University, Canyon, TX, USA
- ^d Mechanical Engineering, Georgia Southern University Statesboro, GA 30458, USA
- ^e Alan G. MacDiarmid NanoTech Institute, University of Texas at Dallas, Richardson, TX 75080, USA

ARTICLE INFO

Keywords: Carbon fiber reinforced polymer composites Carbon nanotubes Molecular dynamics Multi-scale modeling Compressive strength Epoxy

ABSTRACT

The high tensile strength of polymer matrix composites is derived primarily from the high strength of the carbon fibers embedded in the polymer matrix. However, their compressive strength is generally much lower due to the fact that under compression, the fibers tend to fail through micro-buckling well before compressive fracture occurs. In this work, we consider multi-walled carbon nanotube (MWNT) sheets wrapped around carbon fiber at room temperature to improve fiber/matrix interfacial properties which, in turn, influences compressive strength of the composite. To investigate the effect of the wrapping of MWNT sheet on composite strength, Molecular Dynamics simulations were performed on an atomistic model of the interface region between the epoxy, carbon fiber and the scrolled MWNT sheets. The compressive strength of the unidirectional composite was computed using a novel hierarchical multi-scale model comprising of the rule of mixtures at the microscale, and the modified Argon's formula for composites at the macroscale. Model predictions were benchmarked through comparison with experimental data for different volume fractions of MWNT sheet.

1. Introduction

In Polymer Matrix Composites (PMC), the carbon fiber embedded in the matrix provide for the high tensile strength of PMC because of the high strength in tension of the PAN-based carbon fibers. However, under compressive loading, the fibers tend to fail through microbuckling (or kinking) well before the compressive failure, hence resulting in low compressive strength in the PMCs. Also, fiber misalignment and the presence of voids during manufacturing process further reduce the compressive strength. In fact, the overall compressive strength of a unidirectional PMC is only about 50% of the tensile strength, and hence there is much room for improvement [1]. In a composite, load transfer takes place through the interface between the fiber and polymer matrix, and the interfacial region is primarily responsible for shear load transfer and governs the critical buckling load of the fibers by constraining the fibers from buckling [2]. The stiffness and the transfer strength of fiber reinforced composite depends primarily on the thickness of the interface region on the order of 100 nm or less. Swadner et al. [3] determined that the failure or delamination of a glass fiber occur in the matrix at about 3 nm away from the fiber surface. Similar behavior was also observed for Single Walled Carbon Nanotubes (SWNT) nanocomposites. It was also observed by Ding et al. [4] that a small amount of polycarbonate remains wrapped around a SWNT when SWNT is pulled out of polycarbonate matrix during fracture. Therefore, to increase the matrix-dominated properties of composites, such as interfacial shear and compressive strength, it is very important to improve the interfacial mechanical properties by modifying the polymer matrix and/or the interface. In recent years, a lot of effort has been directed towards strengthening the matrix by adding nanofillers to the matrix to make nanocomposites [5,6], or increasing the interfacial stiffness and strength by using Carbon Nanotubes (CNTs) grafted on carbon fibers, sometimes referred to as "fuzzy fibers" [7–18]. However, the process of grafting often leads to degradation of in-plane fiber properties due to the high processing temperatures.

In this paper, we have attempted to resolve the issue using a radically different approach. We spiral wrapped the Multi Walled Carbon Nanotubes (MWNT) sheet around a single carbon fiber or fiber tow with a scrolling (bias) angle α as schematically depicted in Fig. 1 (a) [19].

E-mail address: pkokkadar@ua.edu (P.K. Ravindranath).

^{*} Corresponding author.

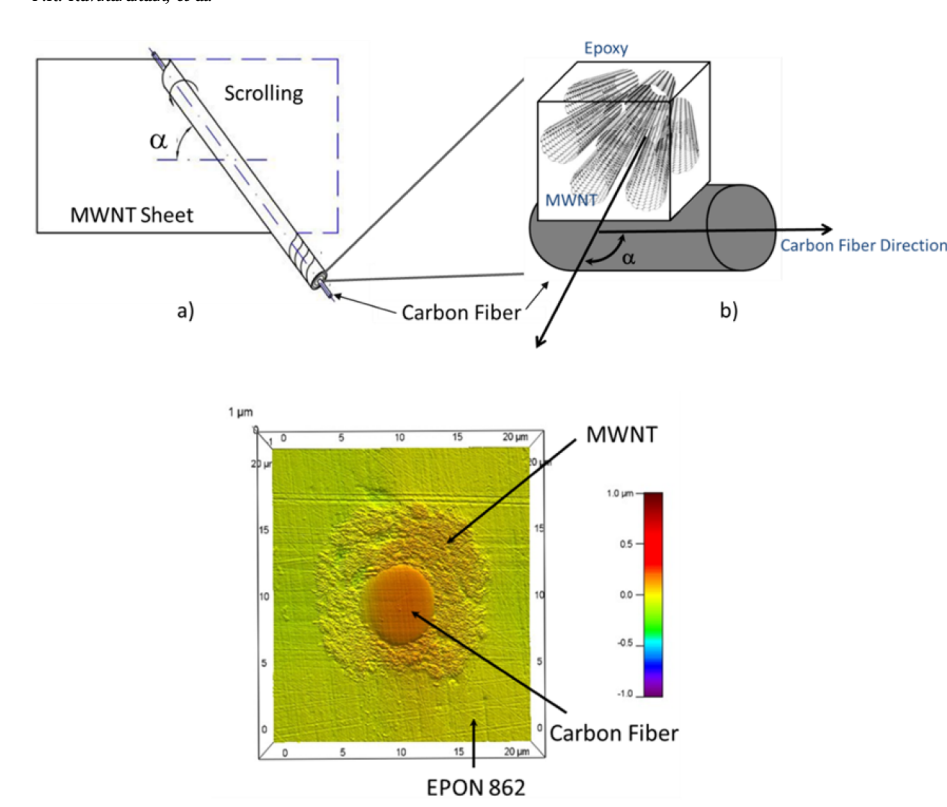


Fig. 1. a) Macroscale view of MWNT sheet scrolled on carbon fiber at a bias angle of α , b) Schematic of nanoscale RVE of the interface region between epoxy-MWNT-carbon fiber showing the bias angle α between MWNT sheet and carbon fiber, c) AFM Image of Epon 862, carbon fiber, MWNT interface (Courtesy: University of Texas-Dallas).

The MWNT sheet overwrapped carbon fiber was subsequently embedded in a polymer matrix, which infiltrates the nanopores of the multilayer MWNT sheet to form mechanically-interlocked MWNT/polymer nanocomposite surrounding the fiber as observed using Atomic Force Microscopy (AFM) as shown in Fig. 1 (c). The relatively high-volume fraction of the MWNT in the matrix provides the reinforcement to the interface region of polymer and fiber due to mechanical interlocking. This approach directly influences the compressive strength of the composite without degrading fiber properties.

c)

2. Overview of the approach

In this paper, our primary focus is to employ multiscale modeling to investigate the enhancement of mechanical properties of the matrix that directly influences the compressive strength of the composite. Our preliminary experimental studies conducted on MWNT sheet wrapped around a tow of carbon fiber at 0° bias angle, showed significant improvement in the polymer shear strength at the interface and compressive strength of the composite ($\sim 80\%$). We developed hierarchical nano-micro-macroscale models to identify the mechanisms that govern compressive strength enhancement in a composite for different MWNT sheet volume fractions, and then validated the model using available test data.

For this purpose, the nano-scale virial stresses in the RVE containing epoxy/MWNT near the carbon fiber interface (shown in Fig. 1 (b)) obtained from MD simulations were used to calculate the composite shear modulus at 50% carbon fiber volume fraction using the rule of mixtures, with and without the MWNTs. Subsequently, the composite shear moduli of the two cases (with and without MWNTs), were incorporated in the modified Argon's formula to calculate the macroscale compressive strength [20]. A full schematic of the three tier nanomicro-macro multiscale modeling approach is shown in Fig. 2, depicting hierarchical coupling of nano, micro, and macro scale modeling.

A step-by-step detail of the hierarchical multiscale modeling scheme is provided in this section.

2.1. Macromechanics

Earlier work by Rosen [2], which assumed extensional (transverse) and shear microbuckling of the fibers imbedded in an isotropic linearly elastic matrix, consistently over-predicted the compressive strength when compared with experimentally measured values. Argon [20] was among the first to recognize that fiber reinforced composites made by standard manufacturing processes, such as VARTM or even pultrusion, have regions of fiber misalignment. Argon [20], and later Budiansky [22,23], showed that fiber misalignments present in fiber reinforced composites could lead to yielding of the polymer matrix during deformation. The yielding of the matrix would, in turn, result in loss of matrix stiffness that could eventually trigger fiber microbuckling and resulting kink band formation leading to final failure [24]. Consequently, it was recognized that the dominant compressive failure mode in continuous fiber polymer matrix composites is localized compressive buckling, or kinking. Argon [20] proposed a simple yet elegant formula for composite strength given by

$$\sigma_{\rm c} = \frac{\tau_{\rm Y}}{\phi_0} \tag{1}$$

where, τ_Y is the matrix yield strength in shear in longitudinal shear, and ϕ_0 is the initial fiber misalignment angle with respect to the load direction, sometimes referred to as fiber misorientation. Subsequently, a modified form of the Argon formula was derived that included both elastic and plastic buckling behavior as limiting cases [24–27],

$$\sigma_{c} = \frac{G_{12c}}{\left(1 + \frac{\phi_{0}}{\gamma_{Y}}\right)} \tag{2}$$

where, G_{12c} is the composite longitudinal shear modulus, and γ_Y is the matrix yield strain in longitudinal shear.

The failure mechanism described in Eq. (2) is still a shear mode of fiber microbuckling, but unlike in Rosen's elastic analysis, it is the local nature of the imperfections, coupled with (perfectly) plastic yielding of

Fig. 2. A schematic diagram showing a nano-micro-macro multiscale approach to calculate the improvement in the Compressive Strength in MWNT scrolled Fiber/Epoxy Composite (Boeing 787 Dreamliner [21]).

the matrix in shear, that results in local microbuckling and kink band formation. From Eq. (2), it is apparent that improvements in the compressive strength of the composite could be achieved by: (a) improving the shear modulus of the matrix surrounding the fiber through the scrolling of MWNT sheets, and (b) by increasing the matrix yield strain in shear through the scrolling of MWNT sheets. Therefore, in this paper, we study the feasibility of this concept through Molecular Dynamics (MD) simulation of the effects of scrolled MWNT sheets that concurrently increases matrix yield strain and matrix shear modulus, thereby making use of synergies that may exist between these effects.

2.2. Micromechanics

The primary purpose of the micro-scale model is to introduce the effects of carbon fiber stiffness and volume fraction into the hierarchical multiscale model. For continuous fiber-reinforced composites, the shear modulus can be calculated using the rule of mixtures which relates to the dependence of the composite shear modulus on shear moduli of the constituent phases and their corresponding volume fractions.

$$G_{12_c} = \frac{G_f G_m}{G_m V_f + G_f V_m} \tag{3}$$

where, G_{12c} is the longitudinal shear modulus of the composite, G_f is the shear modulus of the carbon fiber, G_m is the shear modulus of the matrix (with and without MWNT), and V_f and V_m are fiber volume ratio and the matrix volume fraction, respectively. For this study, a 50% volume fraction of IM7 carbon fiber was assumed with a fiber shear modulus of 14.00 GPa [28]. It should be noted that the assumption that G_{12c} for the composite calculated from the rule of mixtures for the CNT-reinforced polymer in the vicinity of the fiber applies to the entire composite is valid only for high fiber volume fractions due to tight fiber packing with contiguous interface regions (i.e., $V_f > 50\%$). However, this assumption may lead to significant error for resin rich areas and for composites with low fiber volume fraction.

2.3. Nanoscale simulations

The primary purpose of the nano-scale MD model is to incorporate the effects of MWNT/epoxy interface and MWNT volume fraction into the hierarchical multiscale model. A schematic of the RVE in the interface region of the MD model is depicted as a schematic in Fig. 1 (b) in 3-D, and in Fig. 3 (a) in a 2-D view along the MWNT axes. It should be noted that while the presence of the carbon fiber was initially included in the MD model using carbon sheets as shown in Fig. 3 (a), it was later removed from the nanoscale RVE as it resulted in solution instability. The influence of carbon fiber was subsequently included in the model using microscale analysis as discussed earlier. MD simulations were performed to compute the shear modulus for the RVE containing MWNT/epoxy for three cases: (I) baseline epoxy, (II) one MWNT in the RVE (0.0094 volume fraction), and (III) four MWNT in the RVE (0.0376 volume fraction), and are depicted in Fig. 4 (a), (b) and (c), respectively. After proper equilibration of the 3-D MD model, a uniform shear

strain was imposed on the MD box at the operating temperature (300 K) as depicted in Fig. 3 (a) together with periodic boundary conditions on the MD box. The shear stress vs. shear strain curve, as schematically depicted in Fig. 3 (b), was obtained from the simulation of the MWNT/ Epoxy interface region. The matrix shear modulus at the interface (G_m) was computed from the slope of the linear region shear stress vs shear strain curve as depicted in Fig. 3 (b).

For the MD simulations, the open-source LAMMPS software (developed by Sandia Lab) was used. Note that the virial stress for each atom is due to its interaction with all other atoms in the simulation, not just with other atoms in the group. These values of virial stresses for each atom in the system are used to compute the pressure of the entire system of atoms by LAMMPS. A symmetric pressure tensor is computed using the formula:

$$P_{IJ} = \frac{\sum_{k}^{N} m_{k} v_{k_{I}} v_{k_{J}}}{V} + \frac{\sum_{k}^{N} r_{k_{I}} f_{k_{J}}}{V}$$
(4)

here, the first term uses components of the kinetic energy (temperature) and the second term uses components of the virial tensor that includes sum of pair, bonds, angles, dihedrals, improper, K_{space} and fixes contributions to the force on each atom, as discussed above. Because we are concerned only with the Cauchy stress tensor, thermal (residual) stresses were not included in the results.

2.4. Accounting for strain rate effect

A parametric sensitivity study on influence of the strain rate on compressive strength was also performed where the MD models with different MWNT volume fractions were subjected to shear deformation under different strain rates. It was observed that the shear stress-strain response varied for at different strain rates. The behavior of the pure epoxy baseline case, under different strain rates matched very well with the trend of the experimental results by Gilat et al. [27] on the same epoxy system under different strain rates, albeit the experimental strain rates were much lower than the MD strain rates. Using these experimental data in conjunction with the data from MD simulations, a linear relation between the high strain rates and the corresponding shear stress and strain from MD simulations was developed to interpolate shear stress-strain data at high strain rates of MD simulations to the lower strain rates in the experimental regime. A data set at different strain rates is necessary to obtain these parameters over the full strainrate spectrum, as discussed in detail later in this paper. For this work, the strain rates used to obtain these regression parameters ranged between 10^{-3} /s and 10^{12} /s, making use of MD simulation data as well as available experimental data In the linear region of the shear-stress vs. shear strain curve for the isotropic polymer matrix, it is assumed that the shear stress is related to strain via Hooke's law, given by

$$\tau = G_m \gamma \tag{5}$$

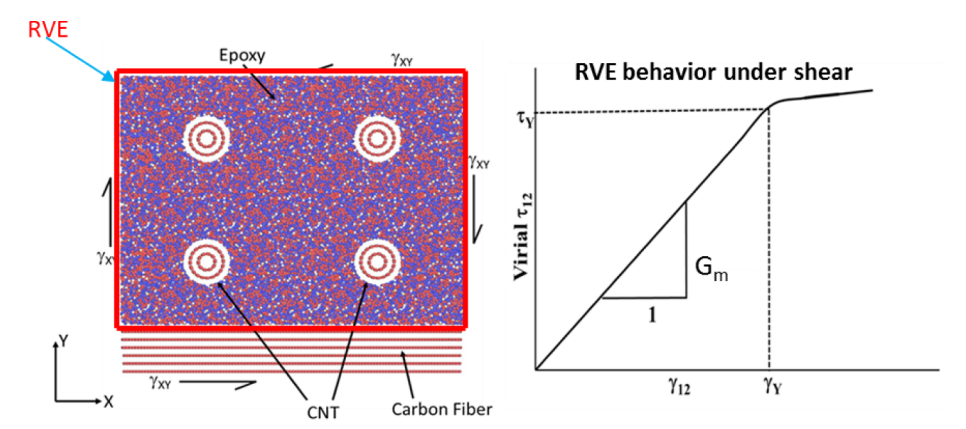


Fig. 3. (a) MD model of MWNT/Epon-862/Carbon Fiber Interface, (b) Virial shear stress vs. strain curve indicating shear modulus and shear strain at yield.

3. Results and discussion

3.1. Computation of compressive strength of unidirectional carbon fiber/epoxy composite

3.1.1. Nanoscale analysis using MD

The reactive force field, ReaxFF (ReaxFF_{C-2013}) [29], was used for all the molecular dynamics (MD) simulations described in this paper, using the open source software, LAMMPS. In ReaxFF the potential energy terms involving the covalent interactions, depends on the bond order function [30]. Bond order function is a continuous function of interatomic distance that, beyond the covalent bond distance, goes to zero. For the work discussed in this paper, two composite material systems were analyzed using MD simulations. The first one being just the Epoxy molecular model, to validate the shear modulus with the experimental results, as shown in Fig. 4 (a), the second being, the interface region between the Epoxy and the Multiwall Carbon Nanotubes (MWNT), as shown in Fig. 4 (b) and (c), for two different MWNT volume fractions. The ReaxFF parameters used for this model are available in literature [31]. The MWNT models were extracted from VMD software (courtesy Sandia Lab). The first system, baseline (Case I), is Epon 862-DETDA polymer, of RVE $13.5 \,\mathrm{nm} \times 10.3 \,\mathrm{nm} \times 6.8 \,\mathrm{nm}$. For the second system, with the MWNT sheet, the same RVE size was maintained. One MWNT was introduced in the epoxy (Case II), by displacing the atoms in the epoxy at a slow increment, until a cylindrical hole of the desired diameter including the van der Waal distance, was achieved. Two concentric carbon nanotubes were introduced in this hole within the epoxy, with chirality (5, 5) and (10, 10) with diameters 0.67 nm and 1.34 nm respectively, as shown in Fig. 4 (b). A similar procedure was followed to introduce four MWNTs (Case III) in the epoxy matrix (Fig. 4 (c)). The length of the MWNTs was 6.8 nm in the z-direction. An important point to note here is that, for all three cases periodic boundary conditions were maintained in all the three directions of x, y and z. The molecular images, as shown in Figs. 3

and 4 were obtained using OVITO molecular graphics software [32]. The density of the baseline system was maintained at $1.224 \, \text{g/cm}^3$, and the system with the MWNTs, was maintained around $1.2 \, \text{g/cm}^3$. The baseline system had an atom count of 102,816 atoms and on the introduction of one and four MWNTs, the atom count increased to 104,436 and 109,536 atoms respectively. A maximum shear strain of about 11-25% was applied to both the baseline system and the MWNT system and the resulting shear stress was computed by LAMMPS using the virial stresses. All simulations were carried out at a room temperature of $300 \, \text{K}$.

For the three nanoscale RVEs under consideration, that is, baseline epoxy and epoxy with one and four MWNT in the interface region, respectively (Fig. 4), the systems were subjected to a maximum shear strain of 25% during the MD simulations at $T = 300 \, \text{K}$. Periodic boundary conditions were used in all cases. Three different strain rates were applied on each of these systems ranging from 2.43×10^{12} to 2.43×10^{10} /s, and it was observed that for each strain rate the individual system response was different, as can be seen in Fig. 5 for baseline epoxy. However, a common trend that was observed among the three systems was that as the applied strain rate was decreased, the maximum shear strength at yield decreased significantly, as did the shear modulus. Fig. 5 shows a compilation of shear stress vs shear strain curves at different strain rates for the baseline epoxy (Case I) obtained from our MD simulations and from published experimental data by Gilat et al. [25]. The experimental strain rates for baseline epoxy ranged between 7×10^2 and 1.3×10^{-3} /s.

Stress-Strain curves similar to the one depicted in Fig. 5 were obtained for Case II (0.0094 volume fraction of MWNT) and Case III (0.0376 volume fraction of MWNT) and are not included in the interest of space. The shear stress vs. shear strain data from these MD simulations and experimental data (shown in Fig. 5) were used to obtain relationships between shear strain at yield (γ_Y) as a function of strain rate using linear regression analysis for strain rates ranging from 10^{-3} to $10^{12}/s$ as shown in Fig. 6 (a). A similar linear regression plot is depicted

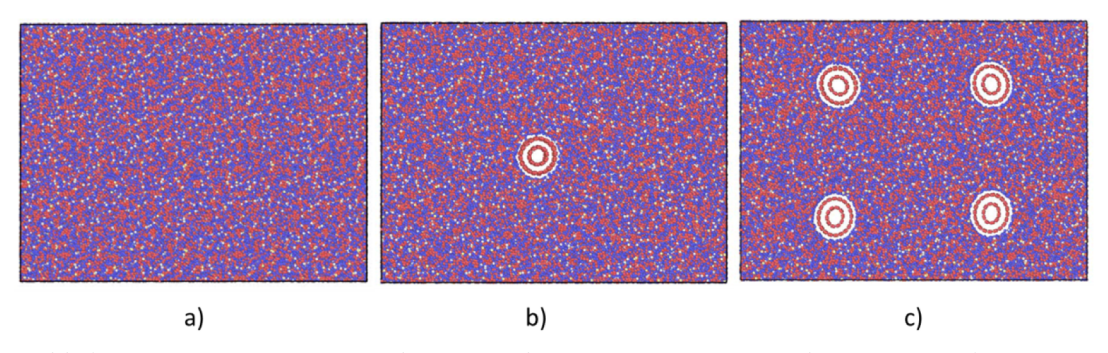


Fig. 4. Molecular Model of (a) Case I: Epon-862 DETDA (Baseline) System, (b) Case II: Epon-862 DETDA with one MWNT interface system (0.0094 MWNT vol. fraction), (c) Case III: Epon-862 DETDA with four MWNTs interface system (0.0376 MWNT vol. fraction).

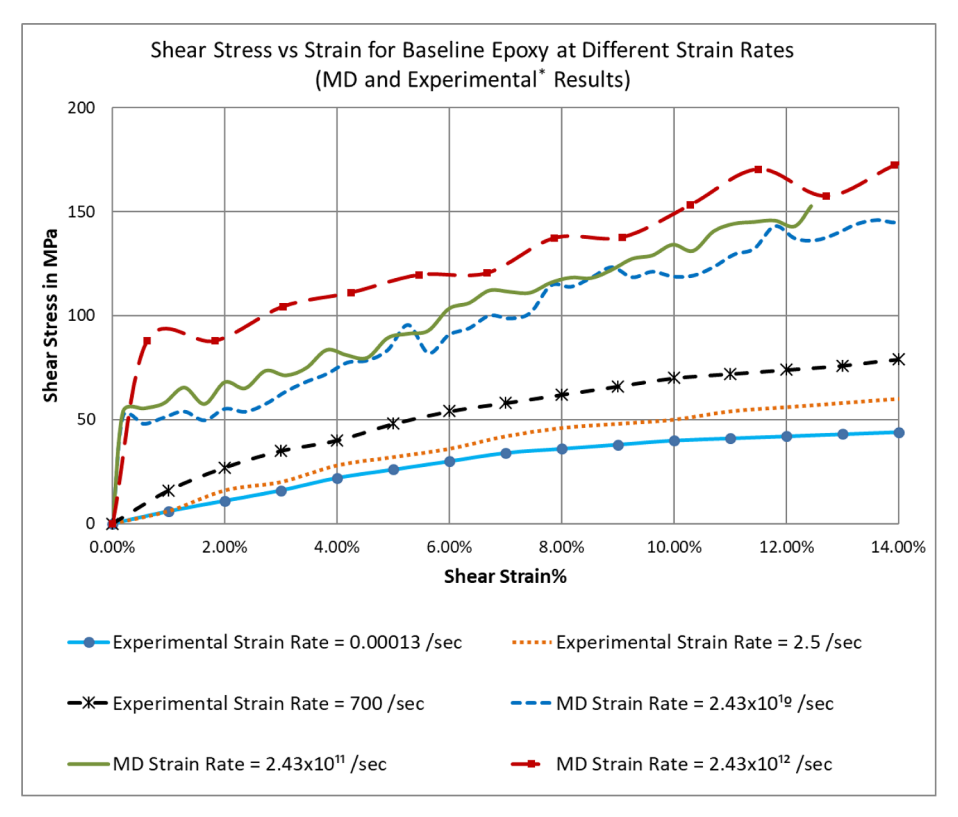


Fig. 5. Shear Stress vs Strain at different strain rates for baseline Epoxy at 300 K.

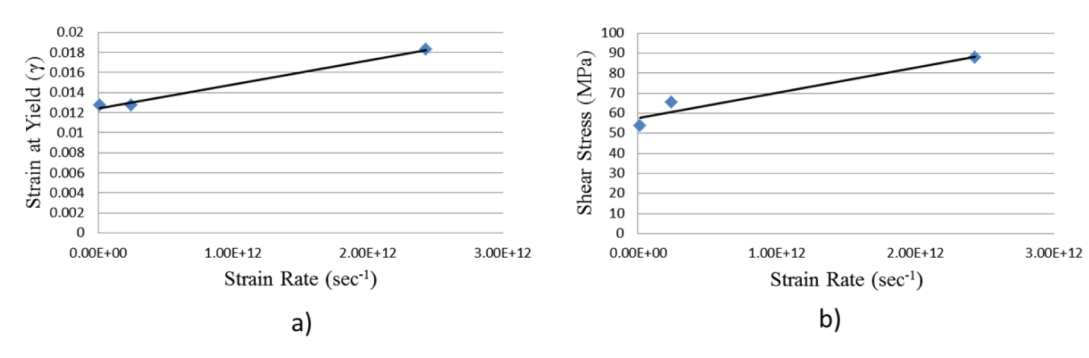


Fig. 6. Linear regression fit as a function of strain rate for baseline epoxy (Case I). a) Shear strain at yield versus strain rates b) Shear strength versus strain rate.

Table 1Compressive Strength of Baseline Epon-862/Carbon Fiber Composite without MWNT from MD Simulations at Different Strain Rates.

	$2.43\times10^{12}/\text{s}$	$2.43\times10^{11}/\text{s}$	$2.43\times10^{10}/\text{s}$	0.01/s
$\gamma_{Y} = \tau_{Y} = G_{m} = G_{f} = V_{f} = G_{12c} =$	0.0182	0.0127	0.0109	0.0124
	88 MPa	65.4 MPa	51.7 MPa	57.8 MPa
	4835 MPa	5149 MPa	4744 MPa	4661 MPa
	14,000 MPa	14,000 MPa	14,000 MPa	14,000 MPa
	0.5	0.5	0.5	0.5
	7188 MPa	7529 MPa	7086 MPa	6993.6 MPa
$\phi_0 = \sigma_c =$	0.1	0.1	0.1	0.1
	1106.7 MPa	848.5 MPa	696.4 MPa	711.6 MPa

in Fig. 6 (b) relating shear stress at yield (τ_Y) to the strain rate. A generally increasing trend with strain rate is observed for both shear stress and shear strain at yield. These data were in turn used to calculate the shear stress and the corresponding shear strain at yield for a nominal strain rate of 0.01/s via interpolation and reported in Table 1. The predicted value of 4.66 GPa for shear modulus of the epoxy resin is considerably higher than the experimentally measured value of 1.25 GPa at low strain rates. A potential reason for this discrepancy is

that the MD model assumes 85% cross-link density and does not include any voids or flaws within the polymer which are likely to exist in a real test specimen [33].

3.1.2. Micromechanical analysis – as alluded to tin the "overview"

These values were used in the Rule of Mixtures for a fiber volume fraction of 50% (Eq. (3)) to obtain the shear modulus, G_{12c} , of the unidirectional composite laminate was calculated, as shown in Table 1. The values used for fiber modulus, matrix modulus, and fiber volume fraction are reported in Table 1.

3.1.3. Macro-scale analysis

Finally, using the value of the longitudinal shear modulus (G_{12c}) of the composite in the modified Argon's formula (Eq. (2)) the compressive strength for the baseline epoxy with 50% fiber volume fraction (Case I) was calculated under different strain rates, as reported in Table 1. A nominal fiber misalignment angle of 0.1 rad was used in all the calculations.

3.2. Methodology for determining compressive strength of unidirectional carbon Fiber/Epoxy composite with MWNT overwrap

As can be observed from Table 1, the predicted value of compressive strength for the carbon-fiber/epoxy composite with baseline epoxy from the multiscale model is 711.6 MPa at a nominal quasi-static strain rate of 0.01/sec, assuming a 50% IM7 fiber volume fraction. This prediction compares reasonably well with the experimentally observed range of 550–800 MPa [1,34] for this material system. The under-prediction of the compressive strength is likely due to a lack of sufficient data for the linear regression analysis in the intermediate strain rate regime.

For the case of MWNT overwrapped carbon fiber (Cases II and III), a similar approach was used to predict the compressive strength of the MWNT scrolled carbon-fiber/epoxy unidirectional composite. First, a parametric study with different MWNT volume fractions was carried out using MD simulations for shear deformation of 11 to 25% and a strain rate range of 2.43×10^{12} – 2.43×10^{10} /s, at a constant operating temperature of 300 K. Similar to the procedure discussed for the baseline epoxy case, linear regression analysis was used to fit the data and the corresponding shear stress and strain at yield were interpolated to obtain shear stress and strain values at a nominal strain rate of 0.01/s. Two MWNT volume fractions were studied, 0.0094 and 0.0376 respectively, which corresponds to one and four MWNT in the RVE, as tabulated in Table 2 and depicted in Fig. 4. The shear stress vs. shear strain results from these MD simulations are plotted and compared in Fig. 7, together with data for baseline epoxy.

Because the volume fraction of MWNT is very low in the epoxy, it was assumed that the strain rate dependence remained the same for the MWNT/Epoxy interface as for the neat epoxy (i.e., Case I) in the low-strain rate regime. Based on this assumption, the compressive strength of the composite laminate for Cases II and III was calculated using the multiscale approach, as reported in Table 2.

As is evident from Table 2, presence of MWNT at 0.0094 volume fraction leads to an improvement in the compressive strength of 21%. Upon increasing the volume fraction of the MWNT to 0.0376 there was a 40% increase in the compressive strength over baseline, indicating a clear correlation between compressive strength of the composite and volume fraction of scrolled MWNT at the fiber-matrix interface region. A 90° degree MWNT scrolling (bias) angle was assumed for all MD simulation.

3.3. Experimental verifications

In this section, verification of the multiscale model is carried out by comparing the MD results was compared with (a) experimental data

Table 2 Compressive Strength Enhancement Comparison on Adding One and Four MWNTs, from MD Simulations, for Shear Deformation Applied at a Strain Rate of 0.01/s.

	Baseline CFRP Case I	CFRP reinforced with one MWNT (0.0094 volume fraction) Case II	CFRP reinforced with four MWNTs (0.0376 volume fraction) Case III
$\begin{array}{l} \gamma_Y = \\ \tau_Y = \\ G_m = \\ G_f = \\ V_f = \\ G_{12c} = \\ \varphi_0 = \\ \sigma_c = \\ \% Improvement \ in \\ compressive \\ strength \ over \\ baseline \ epoxy \end{array}$	0.0124 57.8 MPa 4661 MPa 14000 MPa 0.5 6993.6 MPa 0.1 771.6 MPa	0.015 72 MPa 4800 MPa 14000 MPa 0.5 7148.9 MPa 0.1 932.47 MPa 21%	0.017 86 MPa 5059 MPa 14000 MPa 0.5 7432.3 MPa 0.1 1079.9 MPa 40%

from nanoindentation tests performed at UT-Dallas, and (b) experimental results from three-point bending tests on MWNT wrapped carbon-fiber/epoxy composite beams.

3.3.1. Nanoindentation tests

Nanoindentation tests were performed at UT-Dallas on a single carbon fiber wrapped with CNT sheet and embedded in epoxy matrix. Compressive modulus for the composite with the wrapped CNT sheet (at 0° and 45° bias angle) at different regions of the specimen were obtained using this method as shown in Fig. 8 and as tabulated in Table 3. Oliver-Pharr equation [35] was used to predict the modulus of the composite in the longitudinal direction from the nanoindentation tests.

To compare the compressive modulus from the nanoindentation tests with the MD results, compressive simulations were performed on the nanoscale epoxy-MWNT interface region similar to the RVE shown in Fig. 4, with two different MWNT volume fractions 0.0094 and 0.0376 volume fraction), respectively. A bias angle (α) of 0° was used for the simulation. Comparing computed compressive stress vs. strain data for the two cases of volume fraction at a strain rate of 1.0×10^{10} /s show significant increase in the slope of the stress versus strain plots when the volume fraction of MWNT is increased from 0.0094 to 0.0376 volume fraction as shown in Fig. 9. Compressive stress-strain curves were obtained for these two volume fractions for strain rates ranging from 10^{12} to 10^{10} /s and applying the linear regression approach described in the previous section, the modulus of the epoxy-MWNT interface region was calculated as summarized in Table 4 for the actual nanoindentation strain rate of 0.001/s.

Interpolating these data in Table 4 to 16.1 GPa measured in the nanoindetation test, the estimated volume fraction of MWNT at the fiber-matrix interface in the nanoindentation tests was predicted as 0.0107 volume fraction, or 1.07% by volume.

3.3.2. Three-point bending test of unidirectional IM7/MWNT/epoxy composite beam

The next step was to calculate the relationship between the volume fraction of MWNT and the modulus of the IM7/MWNT/Epoxy composite fiber. For this, a simple micromechanical approach was derived. The first step was to find the relationship between the volume fraction of MWNT wrapped over carbon fiber with the bias angle effect. Fig. 10 depicts the interface region between carbon fiber of radius R_i with wrapped MWNT (embedded in epoxy) at a bias angle α along the carbon fiber longitudinal direction X_I .

Let R_i be the inner radius of MWNT sheet and R_o the outer radius. From micromechanics, assuming iso-strain applied in X_1 direction to the RVE in Fig. 10, the total force is X_1 is:

$$F_1 = E_{MWNT} \pi (R_o^2 - R_i^2) \in_1 + E_F \pi R_i^2 \in_1$$
 (6)

where E_{MWNT} (α) is the elastic modulus of MWNT sheet in X_1 – direction, E_F is the elastic modulus of carbon fiber. But, the total force on the MWNT-carbon fiber interface in the X_1 direction is also given by

$$F_1 = E_{MWNT-CF} \pi R_o^2 \in_1 \tag{7}$$

Equating Eqs. (6) and (7)

$$E_{MWNT-CF} = E_{MWNT}(\alpha) \left(1 - \frac{R_t^2}{R_o^2} \right) + E_F \frac{R_t^2}{R_o^2}$$

$$E_{MWNT-CF} = E_{MWNT}(\alpha) V_{MWNT} + E_F V_F$$
(8)

where, V_{MWNT} is the volume fraction of MWNT and V_F is the volume fraction of carbon fiber. The effect of wrapping angle α (bias angle) on the modulus of the wrapped MWNT ($E_{MWNT}(\alpha)$) can be described by Eq. (9) [1]

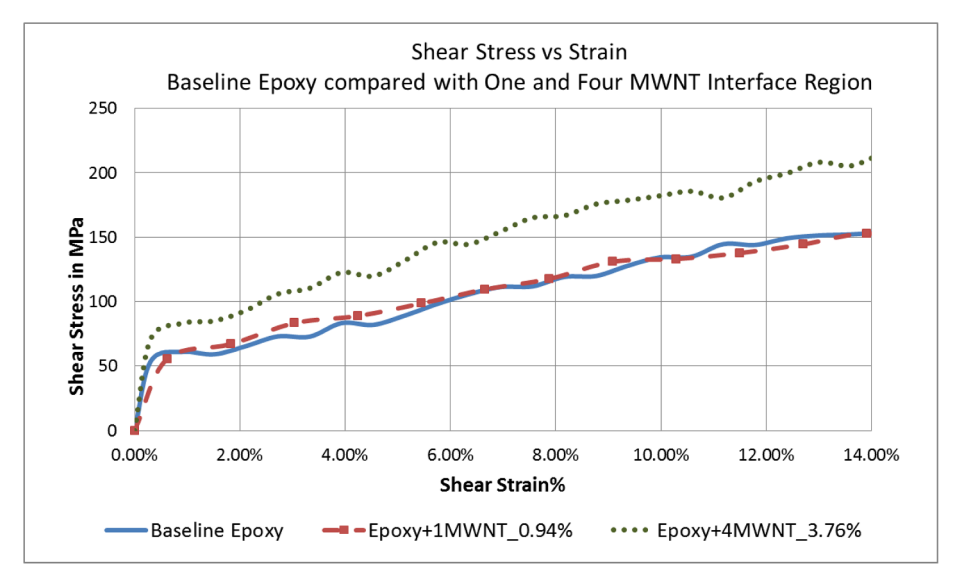


Fig. 7. Shear Stress vs Strain Epoxy/Carbon Fiber/MWNT Interface for different MWNT volume fractions at 300 K and strain rate of $2.43 \times 10^{11}/s$.

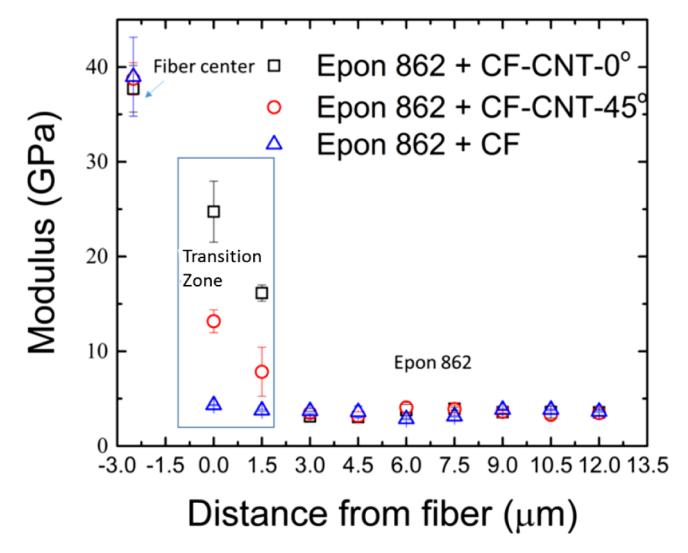


Fig. 8. Modulus estimation from nanoindentation tests (Courtesy: University of Texas-Dallas).

$$\begin{split} \frac{1}{E_{MWNT}(\alpha)} &= \frac{1}{E_{1_{MWNT}}} \cos^4 \alpha + \left[\frac{1}{G_{12_{MWNT}}} - \frac{2\nu_{12}}{E_{1_{MWNT}}} \right] (\sin^2 \alpha) (\cos^2 \alpha) \\ &+ \frac{1}{E_{2_{MWNT}}} \sin^4 \alpha \end{split} \tag{9}$$

At the lamina level, that is, MWNT wrapped carbon fiber sheet embedded in an epoxy matrix, the modulus of the composite was calculated using Eq. (3) (rule of mixtures), where $V_{MWNT-CF}$ is 0.0107 as calculated from the multiscale approach and the nanoindentation results described in the previous section.

$$E_{1_{comp}}(\alpha) = E_{MWNT-CF}(\alpha)V_{MWNT-CF} + E_{M}V_{M}$$
(10)

Equation (10) provides the longitudinal modulus of the composite

laminate and includes the volume fraction of added MWNT at a given bias angle. It was used to compare multiscale model predictions for a three-point bending test for a laminate schematically depicted in Fig. 11, and a relationship between the slope of the load versus deflection of the composite beam was derived as given by Eq. (11):

$$\delta = \frac{-PL^3}{48D_{11}} = \frac{-PL^3}{4b_L h_L^3} \left(\frac{1 - \nu_{12} \nu_{21}}{E_{1_{comp}}(\alpha)} \right)$$
(11)

Defining the slope of $P-\delta$ curve as m,

$$m = \frac{P}{\delta} = \frac{4b_L h_L^3 E_1(\alpha)}{L^3 (1 - \nu_{12} \nu_{21})}$$
 (12)

giving

$$E_{1_{comp}}(\alpha) = \frac{mL^3(1 - \nu_{12}\nu_{21})}{4b_L h_L^3}$$
(13)

Hence, from Eqs. (9) and (10) and (13) the modulus of the composite can directly be related to the volume fraction of MWNT and its bias angle. For a three-point bend specimen with a thickness (h_L) of 0.54 mm, width (b_L) of 4.82 mm and length (L) of 17. 28 mm (from ASTM D7264), the slope of the P/δ curve three-point bend specimen is predicted to be m=2.00. This result does not agree well with the experimentally measured slope of 8.42, from the 3-point bend experiment. The reason for this discrepancy is likely due to the use of the Oliver-Pharr equation [30] for interpretation of the nanoindentation data since the Oliver-Pharr equation has been shown to greatly underpredict the modulus for anisotropic materials.

4. Summary and conclusions

In order to understand the effect of MWNT sheet scrolled carbonfiber on composite strength, a novel hierarchical multi-scale model comprising of MD simulations at the nanoscale, linked to the rule of mixtures analysis at the microscale, linked to the modified Argon's formula for composites at the macroscale, was developed. Model

Table 3 Modulus from Nanoindentation Tests.

Modulus (GPa)	Carbon fiber with wrapped CNT sheet at 0° bias angle embedded in epoxy	Carbon fiber with wrapped CNT sheet at 45° bias angle embedded in epoxy	Baseline
Transition Zone near to fiber	24.7 ± 3.2	13.2 ± 1.2	4.33 ± 0.05
Transition Zone near to Epoxy	16.1 ± 0.9	7.8 ± 2.6	3.76 ± 0.08

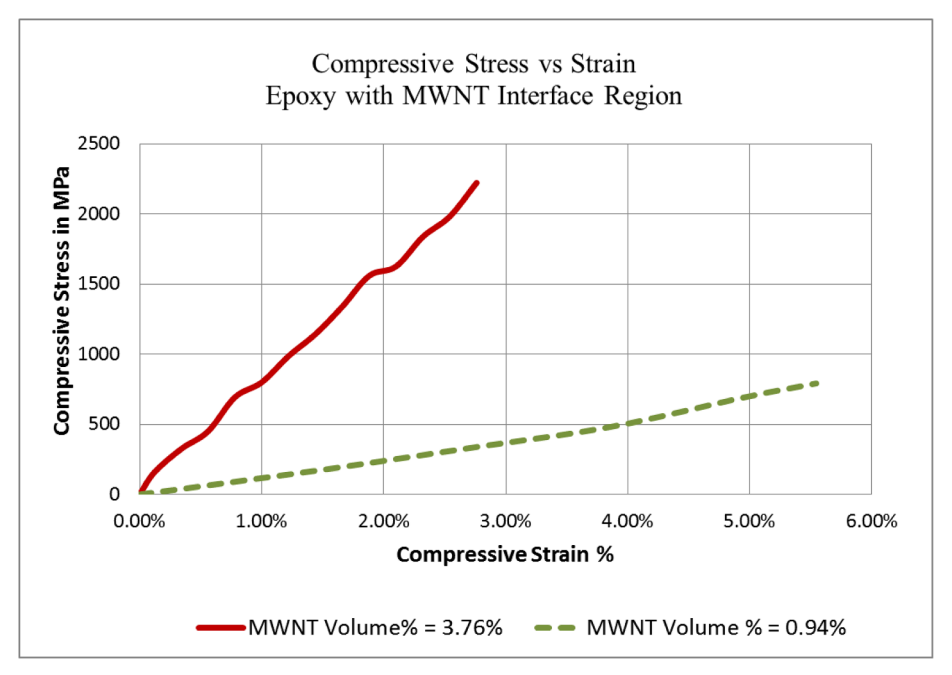


Fig. 9. Compressive Stress vs Strain for epoxy with one and four MWNTs at a strain rate of 1×10^{10} /s at 300 K.

Table 4Modulus of the interface region between epoxy-MWNT from MD simulations and multiscale approach computed at a strain rate of 0.001/s.

% Volume Fraction of MWNT in epoxy	Modulus (GPa)	
0.94%	15	
3.76%	24	

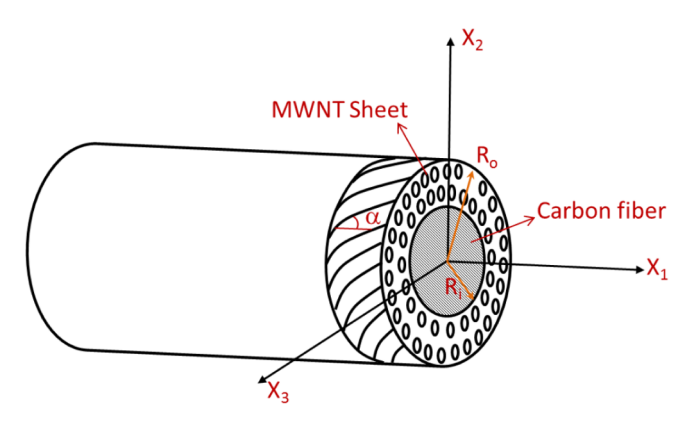


Fig. 10. Schematic of MWNT sheet scrolled single carbon fiber RVE.

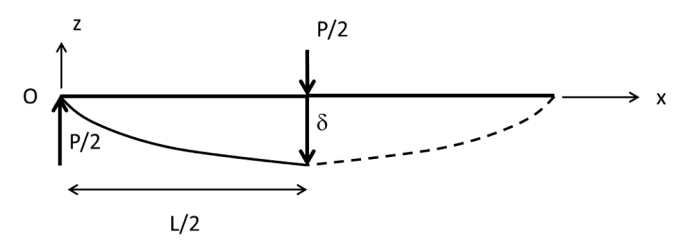


Fig. 11. 3-Point Bending schematic.

predictions were benchmarked through comparison with experimental data baseline case, and for different volume fractions of MWNT sheet. To our knowledge this three-tier multiscale approach has not been used before to predict compressive strength.

At the nanoscale, an atomistic model was developed to study the

interface region between the epoxy (Epon-862), and the scrolled MWNT sheets. Molecular Dynamics (MD) simulations were performed on this model using LAMMPS software to study its behavior under shear deformation. After proper equilibration, a uniform shear strain was imposed on the MD model with the appropriate boundary conditions at room temperature. Shear deformation was applied to the baseline MD model for baseline (without MWNT), for 0.0094 volume fraction MWNT, and for 0.0376 volume fraction MWNT cases. A linear regression analysis was performed to obtain shear stress and shear strain at yield as a function of strain rate.

The predicted compressive strength from the MD results for baseline Epoxy case was shown to be in good agreement with experimental results for unidirectional IM7/Epon-862 composite. Upon adding MWNT sheet at the fiber/matrix interface at different volume fractions, a significant improvement (20–40%) was observed in the compressive strength of the unidirectional composite laminate. Work is currently underway to study the effect bias angle (α) of MWNT sheet on compressive strength prediction.

Acknowledgement

The authors would like to acknowledge the support of this research by the Low Density Materials Program at AFOSR, Grant No. FA9550-14-1-0227 and NSF CMMI-1636308.

Appendix A. Supplementary data

Supplementary data to this article can be found online at https://doi.org/10.1016/j.compstruct.2019.03.065.

References

- [1] Jones RM. Mechanics of Composite Material. 2nd ed. Taylor and Francis; 1998.
- [2] Rosen BW. Mechanisms of composite strengthening, in fiber composite materials. American Society of Metals; 1965. p. 37–75..
- [3] Swadener JG, Liechti KM, Lozanne Ald. The intrinsic toughness and adhesion mechanisms of a glass/epoxy interface. J Mech Phys Solids 1999;47(2):223–58.
- [4] Ding W, et al. Direct observation of polymer sheathing in carbon nanotube polycarbonate composites. Nano Lett 2003;3(11):1593–7.
- [5] Hussain F, et al. Review article: polymer-matrix nanocomposites, processing, manufacturing, and application: an overview. J Compos Mater 2006;40(17):1511–75.

- [6] Thostenson ET, Li C, Chou T-W. Nanocomposites in context. Compos Sci Technol 2005;65(3):491–516.
- [7] Jia J, et al. A comparison of the mechanical properties of fibers spun from different carbon nanotubes. Carbon 2011;49(4):1333–9.
- [8] Frankland SJV, Harik VM. Analysis of carbon nanotube pull-out from a polymer matrix. Surf Sci 2003;525(1):L103–8.
- [9] Qian H, et al. Carbon nanotube grafted carbon fibres: a study of wetting and fibre fragmentation. Compos A Appl Sci Manuf 2010;41(9):1107–14.
- [10] Chowdhury SC, Okabe T. Computer simulation of carbon nanotube pull-out from polymer by the molecular dynamics method. Compos A Appl Sci Manuf 2007;38(3):747–54.
- [11] Sager RJ, et al. Effect of carbon nanotubes on the interfacial shear strength of T650 carbon fiber in an epoxy matrix. Compos Sci Technol 2009;69(7):898–904.
- [12] Fang C, et al. Enhanced carbon nanotube fibers by polyimide. Appl Phys Lett 2010:97(18):181906.
- [13] Grimmer CS, Dharan CKH. Enhancement of delamination fatigue resistance in carbon nanotube reinforced glass fiber/polymer composites. Compos Sci Technol 2010;70(6):901–8.
- [14] Mei L, et al. Grafting carbon nanotubes onto carbon fiber by use of dendrimers. Mater Lett 2010;64(22):2505–8.
- [15] Zhang F-H, et al. Interfacial shearing strength and reinforcing mechanisms of an epoxy composite reinforced using a carbon nanotube/carbon fiber hybrid. J Mater Sci 2009;44(13):3574–7.
- [16] Godara A, et al. Interfacial shear strength of a glass fiber/epoxy bonding in composites modified with carbon nanotubes. Compos Sci Technol 2010;70(9):1346–52.
- [17] Siddiqui NA, et al. Tensile strength of glass fibres with carbon nanotube-epoxy nanocomposite coating. Compos A Appl Sci Manuf 2009;40(10):1606-14.
- [18] Zhang YC, Wang X. Thermal effects on interfacial stress transfer characteristics of carbon nanotubes/polymer composites. Int J Solids Struct 2005;42(20):5399–412.
- [19] Lu H, Baughman R, Haque MH, Fang SD et al. Method of fabricating carbon nanotube sheet scrolled fiber reinforced polymer composites and compositions and uses thereof; 2017. U.S. Patent 20160024262 A1.
- [20] Argon AS. Fracture of Composites. Treatise Mater Sci Technol 1972;1:79-114.
- [21] Archive BI. A Quarterly Publication, Quarter 4, Issue 24. Aero Magazine 2006 06. 28.2017]; Available from: http://www.boeing.com/commercial/aeromagazine/

- articles/qtr_4_06/article_04_2.html.
- [22] Budiansky B. Micromechanics. Comput Struct 1983;16(1):3-12.
- [23] Fleck NA, Budiansky B. Compressive failure of fibre composites due to micro-buckling. In: Dvorak GJ, editor. Inelastic Deformation of Composite Materials: IUTAM Symposium, Troy, New York, May 29 June 1, 1990. New York, NY: Springer New York; 1991. p. 235–73.
- [24] Creighton CJ, Clyne TW. The compressive strength of highly-aligned carbon-fibre/epoxy composites produced by pultrusion. Compos Sci Technol 2000;60(4):525–33.
- [25] Creighton CJ, Sutcliffe MPF, Clyne TW. A multiple field image analysis procedure for characterisation of fibre alignment in composites. Compos A Appl Sci Manuf 2001;32(2):221–9.
- [26] Hussain F, et al. E-Glass—polypropylene pultruded nanocomposite: manufacture, characterization, thermal and mechanical properties. J Thermoplast Compos Mater 2007;20(4):411–34.
- [27] Gilat A, Goldberg Robert K, Roberts Gary D. Strain rate sensitivity of epoxy resin in tensile and shear loading. J Aerosp Eng 2007;20(2):75–89.
- [28] Mechanical Properties of Carbon Fibre Composite Materials, Fibre/Epoxy Resin (120°C Cure). July 2009 14 January 2016].
- [29] Srinivasan SG, van Duin ACT, Ganesh P. Development of a ReaxFF potential for carbon condensed phases and its application to the thermal fragmentation of a large fullerene. J Phys Chem A 2015;119(4):571–80.
- [30] Heyes DM. Pressure tensor of partial-charge and point-dipole lattices with bulk and surface geometries. Phys Rev B 1994;49(2):755–64.
- [31] van Duin ACT, et al. ReaxFF: A Reactive Force Field for Hydrocarbons. J Phys Chem A 2001;105(41):9396–409.
- [32] Alexander S. Visualization and analysis of atomistic simulation data with OVITO-the Open Visualization Tool. Modell Simul Mater Sci Eng 2010;18(1):015012.
- [33] Huang H, Talreja R. Effects of void geometry on elastic properties of unidirectional fiber reinforced composites. Compos Sci Technol 2005;65(13):1964–81.
- [34] Mechanical Properties of Carbon Fiber Composite Materials, Fiber/Epoxy resin; 2009. Performance Composites Ltd.
- [35] Oliver WC, Pharr GM. An improved technique for determining hardness and elastic modulus using load and displacement sensing indentation experiments. J Mater Res 2011;7(6):1564–83.